



28th International Symposium on Superconductivity, ISS 2015, November 16-18, 2015, Tokyo, Japan

## Type-II Superconductivity in Ternary Zirconium Pnictide Chalcogenide Single Crystals

M Baenitz<sup>a\*</sup>, K Lüders<sup>a,b</sup>, R Kniep<sup>a</sup>, F Steglich<sup>a</sup>, M Schmidt<sup>a</sup>

<sup>a</sup>Max-Planck-Institut für Chemische Physik fester Stoffe, Nöthnitzer Str. 40, 01187 Dresden, Germany

<sup>b</sup>Fachbereich Physik, Freie Universität Berlin, Arnimallee 14, 14195 Berlin, Germany

### Abstract

Layered Pnictides are proven to be a great reservoir for superconductors in the past and ternary zirconium pnictide chalcogenides of ZrXY-type ( $X = P, As$ ;  $Y = S, Se$ ) might be a platform for new superconductors. The superconducting properties of carefully grown (chemical transport reaction) single crystals of  $ZrP_{1.54}S_{0.46}$  with a transition temperature of  $T_c = 3.5$  K are investigated. This compound (PbFCl structure type) contains square planar nets: One of the nets is completely occupied (no vacancies) by P, the other one characterized by a random distribution of P and S (full occupation: no vacancies). Besides zero-field-cooling (zfc), field-cooling (fc), and remanent moment (rem) measurements, especially magnetization and ac susceptibility measurements are performed. A nearly ideal type-II behavior with a Ginzburg-Landau parameter  $\kappa = 24$  is found. The magnetization curves between  $B_{c1}$  and  $B_{c2}$  for increasing field are in excellent agreement with theoretical calculations performed by E. H. Brandt based on the Ginzburg-Landau theory. The decreasing branches of the magnetization curves are asymmetric about the field axis indicating weak pinning and also large diamagnetic behavior.

© 2016 The Authors. Published by Elsevier B.V. This is an open access article under the CC BY-NC-ND license (<http://creativecommons.org/licenses/by-nc-nd/4.0/>).

Peer-review under responsibility of the ISS 2015 Program Committee

*Keywords:* Layered Pnictides; Type-II superconductivity

### 1. Introduction

Recently, superconductivity in single crystals of ternary Zr pnictide chalcogenides was reported [1,2]. Depending on the chemical composition the highest superconducting transition temperature of  $T_c = 3.5$  K was found for the

\* Corresponding author. Tel.: +49 351 4646 3217; fax: +49 351 4646 3232

E-mail address: [Michael.Baenitz@cpfs.mpg.de](mailto:Michael.Baenitz@cpfs.mpg.de)

system  $\text{ZrP}_{1.54}\text{S}_{0.46}$  which was established by zfc and fc magnetization data as well as by specific heat measurements, providing evidence for bulk superconductivity in this system. These findings are remarkable in comparison with the behavior of the closely related system  $\text{ZrAs}_{1.58}\text{Se}_{0.39}$  showing superconductivity only at  $T_c = 0.14$  K [1,2]. Both systems crystallize in the tetragonal PbFCl structure type [3].  $\text{ZrAs}_{1.58}\text{Se}_{0.39}$  has about 3 at.% vacancies within the monoatomic As layer, whereas  $\text{ZrP}_{1.54}\text{S}_{0.46}$  contains the P layers without detectable indications for any kind of vacancies. The absence of vacancies in  $\text{ZrP}_{1.54}\text{S}_{0.46}$  might promote the superconductivity in this system.

On the other hand early investigations of the sub-systems Zr-P and Zr-S exhibit superconducting transition temperatures comparable to that of  $\text{ZrP}_{1.54}\text{S}_{0.46}$ . For  $\alpha$ -ZrP transition temperatures from 4.3 to 4.9 K were reported for NaCl-type  $\text{ZrP}_{1.0-0.9}$ . For the system  $\text{Zr}_{0.83-0.85}\text{S}$ , also with NaCl-type structure, transition temperatures from 3.70 to 3.87 K were found [4]. However, the samples used in these investigations, were no single crystals but powdered materials. Although the crystal structures of these binary compounds are different from those of the ternary phases, the atomic distances between Zr and P or S, respectively, are comparable. In the binary compounds the distances are 263 pm for Zr-P and 258 pm for Zr-S [4], whereas in the ternary compound the distance between the Zr- and the P-layers is 260 pm and between the Zr- and P/S-layers is 287 pm. In view of this background it is desirable to get more detailed information on the superconducting properties of  $\text{ZrP}_{1.54}\text{S}_{0.46}$  which are presented in this contribution.

## 2. Experimental

Single crystals of  $\text{ZrP}_{1.54}\text{S}_{0.46}$  are prepared by chemical transport reaction as already described in Ref. [1]. Using a sample with a mass of 10.2 mg zero field cooled (zfc), field cooled (fc), remanent moment (rem), magnetization, and ac susceptibility measurements are performed by means of commercially available magnetometers (MPMS and PPMS, Quantum Design Inc.).

## 3. Results and discussions

### 3.1 Phase diagram

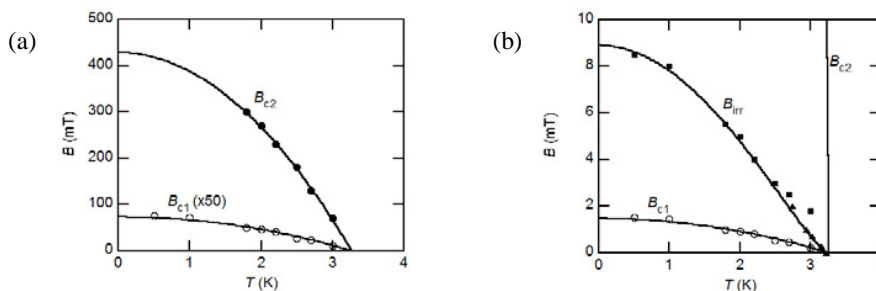


Fig. 1. (a) Field-temperature phase diagram for  $\text{ZrP}_{1.54}\text{S}_{0.46}$ , temperature dependence of the critical magnetic fields  $B_{c1}$  and  $B_{c2}$ ; (b) phase diagram including the irreversibility field  $B_{irr}$ ; (markers for  $B_{irr}$ : triangles: ac measurements, others: magnetization measurements)

Fig. 1(a) shows the temperature dependence of the lower and upper critical field  $B_{c1}(T)$  and  $B_{c2}(T)$  determined from magnetization curves. Within the error bars they follow a quadratic function crossing the temperature axis at the transition temperature  $T_c = 3.2$  K. The onset transition occurs at 3.5 K. Following the expressions connecting the Ginzburg-Landau parameter  $\kappa$  with the ratio of the two critical fields given in Ref. [5], leads to a value of  $\kappa = 24$ . An analysis of the slopes of the magnetization curves at  $T_c$  results in similar values. This  $\kappa$ -value means that there exists a relatively large area in the phase diagram where magnetic flux penetrates into the sample. However, for a rather large part of this area the pinning forces are negligible as can be seen in fig. 1(b), showing in addition to the critical field curves the irreversibility line  $B_{irr}(T)$ . Its values are only larger by a factor of about 5 compared to  $B_{c1}(0)$  but smaller by a factor of nearly 60 compared with  $B_{c2}(0)$ . This means that the system shows nearly ideal type-II superconducting behavior. The temperature dependence of the irreversibility line follows also a quadratic function but with a small correction described by an exponent  $m$ ,  $(1 - (T/T_c)^2)^m$  with  $m = 1.3$ . This leads to a smooth negative bending near  $T_c$  similar to the behavior of high- $T_c$  superconductors [6] which, according to the theory of Matsushita

[7], is based on a depinning mechanism caused by thermally activated flux creep. The deviation of the values determined from magnetization measurements might be due to another pinning mechanism perhaps depending on the grain size which is comparable to the magnetic penetration depth  $\lambda$  in this region.

### 3.2 Magnetization

Fig. 2(a) shows examples of magnetization loops for three different temperatures. The peaks where magnetic flux starts to penetrate into the sample are rather sharp also indicating type-II behavior with very weak pinning. For further analyzing of the magnetization curves the parts between  $B_{c1}$  and  $B_{c2}$  are considered. As example the curve for the temperature 1.8 K is shown in fig. 2(b). The magnetic moment  $-M$  is normalized to its maximum value  $B_{c1}$  occurring at  $b = B/(B_{c2} - B_{c1})$  on the horizontal axis, where  $b^{0.5}$  is plotted in order to stretch the low field region. Such plots can be compared with theoretical expressions calculated by E.H. Brandt [5] from the Ginzburg-Landau theory for the entire range of fields between  $B_{c1}$  and  $B_{c2}$  and a set of Ginzburg-Landau parameters between  $\kappa = 0.85$  and  $\kappa = 200$ . In the figure the prediction for  $\kappa = 24$  is plotted which leads to a very good agreement with our experimental data. This means, that the field inside the sample corresponds to an ideal triangular vortex lattice.

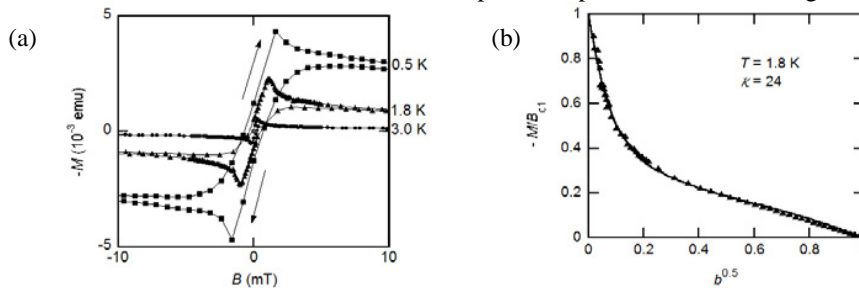


Fig. 2. (a) Central parts of magnetization loops for three different temperatures; (b) magnetization data for 1.8 K between  $B_{c1}$  and  $B_{c2}$  in comparison with the prediction calculated from the Ginzburg-Landau theory [5]

### 3.3 Ac susceptibility

In order to get more information about the vortex dynamics ac susceptibility measurements are performed. The temperature dependence of the real and imaginary parts of the ac susceptibility,  $\chi'$  and  $\chi''$ , was recorded in magnetic fields up to 3 mT. Frequency and ac field amplitude were fixed to 1 kHz and 0.1 mT, respectively. Fig. 3(a) shows some results. Comparing the applied magnetic fields with the phase diagram in fig. 1(b) shows that the curves for 2 and 3 mT do not enter the Meissner phase below  $B_{c1}$ . For further analysis the ac results are used which are obtained for the fields where the zero field state is reached at the temperature of 1.8 K (0.27, 0.7, and 1.0 mT in fig. 3(a)). The imaginary parts of the ac susceptibility are plotted against their real parts (fig. 3(b)). The peak heights of  $\chi''$  are about 0.24 if the minimum values of  $\chi'$  are normalized to  $-1$ . So this plot shows the behavior of the transition region from the field to the zero field state. This kind of plot can be compared with theoretical predictions [8] based either on Bean's critical state model or another model based on diffusive motion of the flux lines, both indicated in the figure. Only at temperatures very near to the onset temperature to superconductivity the experimental values seem to correspond to the model of diffusive motion. Mainly, however, their behavior agrees well with the prediction of the critical state model.

### 3.4 Zfc, fc, and rem measurements

Zero field cooled (zfc), field cooled (fc), and remanent moment (rem) measurements are performed in different applied magnetic fields (0.12, 0.335, 0.5, 1.0, and 5.0 mT). These field values are similar to the variety of fields applied in the ac measurements in order to allow comparisons of the results of both methods. In agreement with the ac results the zfc curves show that for applied fields below  $B_{c1}$  (at 1.8 K below 1.0 mT) complete flux expulsion is reached. With increasing temperature flux penetration occurs earlier in higher applied magnetic fields. However, the

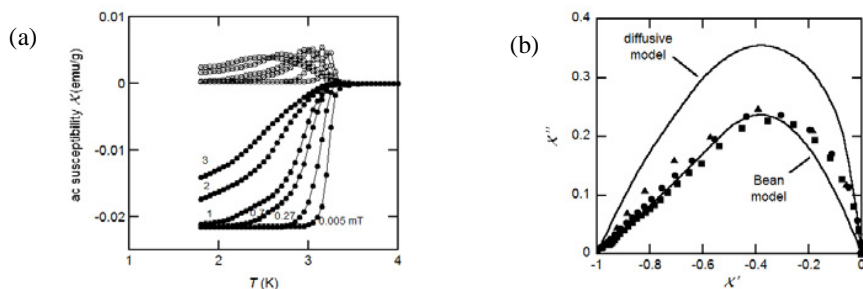


Fig. 3. (a) Real parts  $\chi'$  (closed symbols) and imaginary parts  $\chi''$  of the ac susceptibility for different applied magnetic fields; (b)  $\chi''$  plotted against  $\chi'$  for three fields in the low field region compared with theoretical predictions (triangles: 0.27, circles: 0.7, squares: 1.0 mT)

magnetic moments at 1.8 K (measured at the three magnetic fields 0.12, 0.335, and 0.5 mT) are not proportional to these field values. An extrapolation to zero shows that their zero line occurs at about  $-0.02$  emu/g ( $\approx 4\%$  of the magnetic moment at 0.12 mT). This indicates an additional diamagnetic contribution which obviously is due to shielding currents localized in the surface region of the sample. This effect of diamagnetism cannot be neglected in superconductors in which the pinning force is weak [9] which is reasonable in our case. Also the fc and rem behavior supports such diamagnetism conspicuously. For both groups of curves the extrapolated zero line differs from the real zero line: for the fc curves at their merging points and for the rem curves at the point where the sign of the slope is changing. At temperatures above these points only this diamagnetic contribution is responsible for the measured magnetic moments, whereas below these points in addition the flux line caused diamagnetism (fc) or paramagnetism (rem), respectively, is present.

#### 4. Conclusions

Single crystals of the layered zirconium pnictide chalcogenide  $\text{ZrP}_{1.54}\text{S}_{0.46}$  exhibit superconductivity below 3.5 K. According to magnetization, ac susceptibility, zfc/fc, and rem measurements the material can be classified as a nearly ideal type-II superconductor. In the mixed state the magnetization follows the prediction of the Ginzburg-Landau theory with a  $\kappa$ -value of 24. The corresponding area in the phase diagram is relatively large with only weak pinning forces. Furthermore the ac susceptibility behavior agrees well with the prediction of Bean's critical state model. The presence of weak pinning is also supported by an additional diamagnetic contribution observed in the zfc/fc and rem measurements. In comparison with other Zr pnictide chalcogenides it is obvious that the absence of vacancies in  $\text{ZrP}_{1.54}\text{S}_{0.46}$  is essential for its superconducting properties.

#### Acknowledgements

We would like to thank H. Rave for experimental help and T. Cichorek for fruitful discussions. One of us (KL) would like to thank F. Steglich and A.P. Mackenzie for their kind hospitality and the possibility of doing research at the MPI-CPfS.

#### References

- [1] T. Cichorek, L. Bochenek, A. Czulucki, M. Schmidt, R. Niewa, G. Auffermann, Y. Prots, R. Wawryk, M. Baenitz, F. Steglich, R. Kniep, Scientific Report MPG/CPfS (2011) 103 ([www.cpfis.mpg.de/2081022/B\\_2009-2010.pdf](http://www.cpfis.mpg.de/2081022/B_2009-2010.pdf)).
- [2] T. Cichorek, to be published.
- [3] A. Schlechte, R. Niewa, M. Schmidt, G. Auffermann, Y. Prots, W. Schnelle, D. Gnida, T. Cichorek, F. Steglich, R. Kniep, Sci. Techn. Adv. Mater. 8 (2007) 341.
- [4] A.R. Moodenbaugh, D.C. Johnston, R. Viswanathan, R.N. Shelton, L.E. DeLong, W.A. Fertig, J. Low Temp. Phys. 33 (1978) 175.
- [5] E.H. Brandt, Phys. Rev. B 68 (2003) 054506.
- [6] P. Schilbe, K. Lüders, M. Baenitz, D.A. Pavlov, A. Abakumov, E.V. Antipov, Physica C 388-389 (2003) 247.
- [7] T. Matsushita, Physica B 164 (1990) 150.
- [8] X. Ling, J.I. Budnick, in R.A. Hein, T.L. Francavilla, D.H. Liebenberg (Eds.), Magnetic Susceptibility of Superconductors and other Spin Systems, Plenum Press, New York and London, 1991, p. 377.
- [9] T. Matsushita, Flux pinning in superconductors, second ed., Springer, Berlin Heidelberg, 2014, Sec. 2.6.